Advanced Engineering Informatics 37 (2018) 163–174

Contents lists available at ScienceDirect

Advanced Engineering Informatics

journal homepage: www.elsevier.com/locate/aei

Review article

A review of 3D reconstruction techniques in civil engineering and their applications

Zhiliang Ma*, Shilong Liu

Department of Civil Engineering, Tsinghua University, Beijing, China

ARTICLE INFO

Keywords:
3D reconstruction techniques
Civil engineering
Point clouds
Achievements
Challenges

ABSTRACT

Three-dimensional (3D) reconstruction techniques have been used to obtain the 3D representations of objects in civil engineering in the form of point cloud models, mesh models and geometric models more often than ever, among which, point cloud models are the basis. In order to clarify the status quo of the research and application of the techniques in civil engineering, literature retrieval is implemented by using major literature databases in the world and the result is summarized by analyzing the abstracts or the full papers when required. First, the research methodology is introduced, and the framework of 3D reconstruction techniques is established. Second, 3D reconstruction techniques for generating point clouds and processing point clouds along with the corresponding algorithms and methods are reviewed respectively. Third, their applications in reconstructing and managing construction sites and reconstructing pipelines of Mechanical, Electrical and Plumbing (MEP) systems, are presented as typical examples, and the achievements are highlighted. Finally, the challenges are discussed and the key research directions to be addressed in the future are proposed. This paper contributes to the knowledge body of 3D reconstruction in two aspects, i.e. summarizing systematically the up-to-date achievements and challenges for the applications of 3D reconstruction techniques in civil engineering, and proposing key future research directions to be addressed in the field.

1. Introduction

Three-dimensional (3D) reconstruction is the process of generating 3D representations of the 3D appearance of objects from the outputs of data collection equipment [1,2]. Generally, the 3D representations are in the form of point cloud models, mesh models and geometric models, among which, point cloud models are the basis. Because the techniques are both efficient and cost-effective [3] for obtaining 3D representations of objects, they have been applied in many fields, such as surveying engineering [4], medical engineering [5]. In recent years, they have been applied in civil engineering as well. For example, the 3D models generated from applying the techniques have been used for the preservation of historical buildings [6–8], for analyzing the energy efficiency of buildings [9], and for acquiring the surface texture of pavements [10]. However, such applications are still in the early stage and it is anticipated that their potential is large. To enhance such applications, it is essential to clarify the status quo of the research and application of the techniques through literature review.

3D reconstruction techniques in civil engineering and their applications have been summarized in a number of review papers. Tang et al. [11] summarized the 3D reconstruction techniques for creating as-built building information models (BIM) through the point clouds from laser scanners. Lu and Lee [3] reviewed the image-based techniques for constructing as-is BIM for existing buildings. But in the two reviews, they did not go to the detailed process of some steps, such as point cloud preprocessing and mesh reconstruction. In addition, they confined their target objects to only buildings. Parn and Edwards [12] reviewed the principles, cost, specifications and applications of laser scanning, i.e. progress tracking, quality assessment, structural health monitoring and creating as-built BIM. Son et al. [13] reviewed the applications of the 3D reconstruction techniques based on photos, videos and laser scanning, i.e. dimensional quality control, progress tracking and reconstruction of Mechanical, Electrical and Plumbing (MEP) systems.

The other techniques that are relevant to 3D reconstruction techniques in civil engineering and their applications, have also been summarized in some publications. Teizer [14] summarized the computer vision based personnel tracking, equipment tracking and detection on construction sites. Koch et al. [15] reviewed the computer vision based defect detection and condition assessment of civil infrastructure, including reinforced concrete bridges, precast concrete tunnels, underground concrete pipes and asphalt pavements. Koch et al.

* Corresponding author.
E-mail address: mazl@tsinghua.edu.cn (Z. Ma).

https://doi.org/10.1016/j.aei.2018.05.005
Received 30 September 2017; Received in revised form 4 March 2018; Accepted 17 May 2018

[16] presented current achievements and open challenges in the machine vision-based inspection of large concrete structures. In all these three reviews, 3D reconstruction techniques were involved as one of the methods. Mathavan et al. [17] reviewed the 3D imaging-based technologies for pavement distress detection and measurements, where 3D reconstruction-related techniques including stereo imaging, laser scanning and structured light systems are involved.

In the above-mentioned review papers, two important aspects about 3D reconstruction techniques are missing: (1) some important steps for 3D reconstruction techniques, including feature matching, camera motion estimation and absolute scale recovery; (2) the key research directions of the techniques and their applications in the future. Among them, the steps in the former aspect have been regarded to be indispensable in a specific research [18], while the latter aspect is obviously important to the civil engineering community. Taking into account of such limitations, this paper systematically summarizes 3D reconstruction techniques and the up-to-date achievements and challenges for the applications of the techniques in civil engineering and proposes key future research directions in the field.

The remainder of this paper focuses on the process, algorithms and methods of 3D reconstruction techniques, and their achievements and challenges in civil engineering. In Section 2, the methods used for literature retrieval and for determining the research scope are introduced, and the framework of the techniques in civil engineering is illustrated. Sections 3 and 4 present the techniques for 3D reconstruction, including the techniques for generating point clouds and that for processing point clouds respectively, particularly the corresponding algorithms and methods. Section 5 presents the applications of the techniques in reconstructing and managing construction sites and reconstructing pipelines of MEP systems as typical examples, and highlights the achievements. Section 6 discusses the challenges of applying the techniques in civil engineering and proposes the key research directions to be addressed in the future. Section 7 concludes the paper.

2. Methodology

2.1. Literature retrieval conditions

The major databases in the world, including Web of Science, Engineering Village and China Knowledge Resource Integrated Database, are retrieved by using keywords including '3D reconstruction', 'three-dimensional reconstruction', 'three dimensional reconstruction' and '3-D reconstruction' to obtain a list of publications dating from 2000 to the present. Since the keywords do not confine the target objects of the research and application of 3D reconstruction techniques in civil engineering, these publications are then filtered through reading the abstracts to exclude those that are not related to the areas of civil engineering.

2.2. Research scope

By analyzing the publications obtained from Section 2.1, 95 publications in total, the frequency of publications in terms of data collection equipment types is shown in Table 1.

It deserves to explain that laser scanners are also known as Light Detection And Ranging (LiDAR) [18,19]. Because the phrase 'laser scanners' is more frequently used than the word 'LiDAR' in the reviewed publications, 'laser scanners' is chosen to be used from here on in this paper.

According to the table, monocular cameras, binocular cameras, video cameras and laser scanners have been used with high frequency for 3D reconstruction techniques in civil engineering, while CT, ultrasonic tomography, Kinect and total stations have been rarely used. In order to focus on the major 3D reconstruction techniques, only the techniques that are applied in civil engineering and based on the following data collection equipment, i.e. monocular cameras, binocular cameras, video cameras and laser scanners, are reviewed in this paper.

Table 1
The frequency of publications in terms of data collection equipment types per five years since 2000.

Data collection equipment types	2000–2004	2005–2009	2010–2014	2015-prseent	Total
Monocular cameras	–	4	22	15	41
Binocular cameras	–	3	3	3	9
Video cameras	–	2	7	1	10
Laser scanners	–	3	15	9	27
Computerized Tomography (CT)	–	1	1	2	4
Ultrasonic tomography	1	–	–	1	2
Kinect (based on structured light)	–	–	–	1	1
Total stations	–	–	1	–	1
Total	1	13	49	32	95

The 3D reconstruction techniques based on monocular cameras, binocular cameras and video cameras can be classified into two categories according to their principles, i.e. point-based ones and line-based ones. In the former, the feature points in the outputs of monocular cameras, binocular cameras and video cameras are extracted and processed in subsequent steps [19–21], while in the latter, the feature lines in the outputs of monocular cameras, binocular cameras and video cameras are extracted and processed in subsequent steps [22–27]. Because the latter category of 3D reconstruction techniques has very few applications up to now, this category is not reviewed in this paper.

In case some algorithms and methods need to be quoted, other publications except the 95 publications have also been cited in this paper, for example, the publication on Scale Invariant Feature Transform (SIFT) algorithm.

2.3. Framework of 3D reconstruction techniques in civil engineering

Through reviewing the selected publications, the framework of 3D reconstruction techniques in civil engineering is established as shown in Fig. 1.

In the framework, the 3D reconstruction techniques are divided into two big steps, i.e. generating point clouds and processing point clouds, and each big step can be further divided into several steps. In the former big step, the outputs of monocular cameras, binocular cameras and video cameras are processed to generate the point clouds corresponding to a certain scene. In the latter big step, point clouds obtained from the previous big step or that from laser scanners are processed to generate the outputs of 3D reconstruction techniques for the objects of interest in the scene. In order to make it easy to read, the 3D reconstruction techniques will be reviewed in this big step-and-step framework, with Sections 3 and 4 dedicated to the two big steps, respectively.

3. Techniques for generating point clouds

In general, the inputs of 3D reconstruction techniques are the outputs of data collection equipment. The inputs of the techniques with high frequency in civil engineering are monocular images, stereo images, video frames and point clouds, corresponding to monocular cameras, binocular cameras, video cameras and laser scanners, respectively. It deserves to explain, although monocular images, stereo images and video frames are all digital images, they have different characteristics. Indeed, stereo images contain monocular images in pair, while video images contain a series of monocular images, or a series of stereo images. In this section, the processes of generating point clouds from monocular images, stereo images and video frames and algorithms and methods used in these processes are presented. Since the

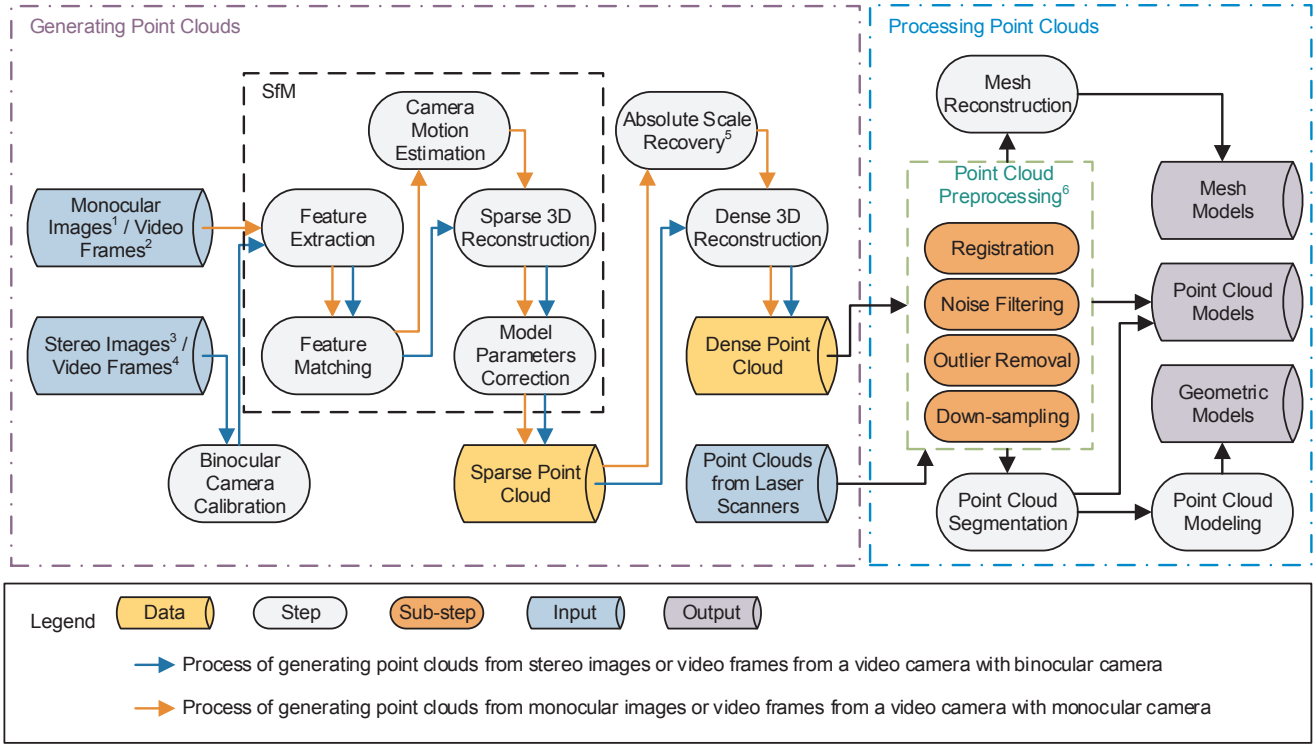

Fig. 1. The framework of 3D reconstruction techniques in civil engineering. Note: 1-generated from monocular cameras; 2-generated from a video camera with monocular camera; 3-generated from binocular cameras; 4-generated from a video camera with binocular cameras; 5-the step is not mandatory in some cases; 6-sub-steps here are not mandatory, and which sub-steps are needed depend on the application requirements and the quality of the point clouds.

outputs of laser scanners are point clouds, laser scanners are not discussed in this section.

3.1. Generating point clouds from monocular images

According to the publications, the process of generating point clouds from monocular images slightly differs from each other. Generally, the process consists of seven steps, i.e. feature extraction, feature matching, camera motion estimation, sparse 3D reconstruction, model parameters correction, absolute scale recovery and dense 3D reconstruction, as shown in Fig. 1. Normally, the combination of the steps of feature extraction, feature matching, camera motion estimation, sparse 3D reconstruction and model parameters correction is called Structure from Motion (SfM) [28,29], as shown in Fig. 1. Each step from the second step needs to use the result obtained from the previous steps as the input. The algorithms and methods used in each step are shown in Table 2.

3.1.1. Feature extraction

The aim of the step is to gain feature points, which reflect the initial structure of the scene [18], from the images of a certain scene. The algorithms used for the step can be divided into two categories, i.e., feature point detectors, which obtain the locations of feature points of an image, and feature point descriptors, which generate the vectors or strings to characterize the feature points detected by feature point detectors.

The feature point detectors used for the step are SIFT detector, Speeded-Up Robust Features (SURF) detector, Affine Scale Invariant Feature Transform (ASIFT), Harris corner detector and Features from Accelerated Segment Test (FAST). In SIFT detector [30], a scale space, containing images with different scale, is generated from an initial image by Gaussian convolution, and adjacent images in the scale space are subtracted to produce difference-of-Gaussian images. Then the feature point candidates are found by comparing each pixel to its neighbors in the difference-of-Gaussian images. After that, feature points are obtained by refining feature point candidates. In SURF detector [31,32], a scale space is generated based on integral images, and the approximated determinant of the Hessian of each pixel in the scale space is calculated. Then feature points are found based on the approximated determinant of the Hessian of each pixel. ASIFT [33] is the variation of SIFT detector. In this algorithm, simulated images of each initial image with all possible distortions caused by the change of the camera optical axis orientation are generated. Then all simulated images are processed by SIFT detector to find feature points. Therefore, for images with viewpoint changes, more feature points can be extracted by using ASIFT than SIFT detector [34]. Harris corner detector [35] detects corners based on the image intensities change around each pixel on the images. FAST [36] is a corner detector faster than Harris corner detector, and it identifies a pixel as a corner if the number of pixels in the circle consisting of sixteen pixels around the pixel meets the threshold.

The feature point descriptors used for the step are SIFT descriptor, SURF descriptor, Fast REtinA Keypoint (FREAK) and Multi-Scale Descriptor (MSD). SIFT descriptor [30] generates a vector for characterizing a feature point based on computing the gradient magnitude and orientation at each image point in a region around the feature point. SURF descriptor [31] generates a vector for characterizing a feature point based on computing the Haar-wavelet responses in a region around the feature point. FREAK [37] is a coarse-to-fine feature point descriptor, and the outputs of the descriptor is a binary string based on retinal sampling pattern formed by a sequence of one-bit difference of Gaussians. MSD [38] generates a vector for characterizing a feature point based on the intensity gradients over multiple scales. The comparison on robustness and speed for generating vector among these feature point descriptors is shown in Table 3.

3.1.2. Feature matching

The aim of the step is to match the feature points of each image pair

Table 2
Algorithms and methods used in the steps for generating point clouds.

Inputs	Steps	Algorithms and methods
Monocular images/video frames[1]	Feature extraction	SIFT [28,39–43] (including SIFT detector and SIFT descriptor); SURF [21] (including SURF detector and SURF descriptor); ASIFT [44]; FREAK [45]; Harris corner detector [38]; FAST [38]; MSD [38]
	Feature matching	RANdom SAmple Consensus (RANSAC) [40,43,46–48]; Optimized Random Sampling Algorithm (ORSA) [44]; Approximate Nearest Neighbors (ANN) [29,45]; Fast Library for Approximate Nearest Neighbors (FLANN) [43]
	Camera motion estimation	Direct Linear Transform (DLT) [40,49]; Five-point algorithm [45,49]; Eight-point algorithm [21,44,50]
	Sparse 3D reconstruction	Triangulation [28,29,38,43]
	Model parameters correction	Bundle Adjustment (BA) [28,41,43–45];
	Absolute scale recovery	Geo-registration [51,52]; Recovering manually [53]; Recovering by premeasured objects [53]
	Dense 3D reconstruction	Clustering Multi-View Stereo (CMVS) [28,29,54]; Patch-based Multi-View Stereo (PMVS) [29,44,53,55,56]; Semi-Global Matching (SGM) [43,57]
Stereo images/video frames[2]	Binocular camera calibration	Two-step procedure [20,58]

[1] Generated from a video camera with monocular camera.
[2] Generated from a video camera with binocular cameras.

Table 3
Comparison among feature point descriptors [21,37,38,48,59].

Descriptors[1]	Dimensions of Vector	Robustness
SIFT descriptor	128	Robust to scale, rotation and translation changes
SURF descriptor	64	Robust to scale and rotation changes
FREAK	–[2]	Robust to scale and rotation changes
MSD	108	–

[1] The comparison on the speed for generating vectors or strings among the feature point descriptors: SURF descriptor is faster than SIFT descriptor [21,37,48,59], FREAK is faster than SUFR descriptor [37] and MSD is faster than SUFR descriptor [38,59].
[2] The output of FREAK is a binary string.

and remove false matches by using the feature points obtained from the previous step to obtain correspondences among the features points.

ANN is used to match the feature points of each image pair by computing the Euclidian distance of feature point descriptors across two images [18]. The outputs of ANN are matched feature points, but false matches may exist in the result because the criterion of matching feature points is only relevant to the Euclidian distance of feature point descriptors and it loses sight of the epipolar geometry of the image pair, which describes the uniqueness of the matched feature points in each image pair. The function of FLANN is similar to that of ANN [43], but it is faster than ANN due to its approximate nearest neighbor search algorithm [60].

RANSAC is used to remove false matches by utilizing the epipolar geometry of an image pair. In the algorithm, the epipolar geometry is estimated by random sampling of matched feature points iteratively [61] rather than by all the matched feature points, which can mitigate the effort of false matches. ORSA is the variant of RANSAC [44], and it can remove false matches more effectively than RANSAC when false matches are more than 50 percent [62].

3.1.3. Camera motion estimation

The aim of the step is to find out camera parameters of each image, including intrinsic parameters (e.g., focal length and radial distortion) and extrinsic parameters (i.e. rotation and translation) by using the feature points of each image pair.

In the epipolar geometry of an image pair, two matrixes can be used respectively to describe the correspondences between the matched feature points of the image pair, i.e., essential matrix and fundamental matrix. The essential matrix [63], which contains extrinsic parameters, describes the correspondences between the matched feature points of camera coordinates, while the fundamental matrix [63], which contains intrinsic and extrinsic parameters, describes the correspondences between the matched feature points of pixel coordinates. In the five-point algorithm [64], the essential matrix is computed based on five matched feature points, and the extrinsic parameters, i.e. rotation matrix and translation matrix, are obtained based on the singular value decomposition of essential matrix. In the eight-point algorithm [65], an initial fundamental matrix is computed based on eight matched feature points by linear solution, then a new fundamental matrix is computed based on singular value decomposition to replace the initial fundamental matrix, which ensures that the fundamental matrix is singular. Typically, the five-point algorithm is used to compute extrinsic parameters, while the eight-point algorithm is used to compute intrinsic and extrinsic parameters. In another word, the five-point algorithm is preferable when the intrinsic parameters are known and the aim is to compute extrinsic parameters, while the eight-point algorithm is preferable when the aim is to compute extrinsic parameters and intrinsic parameters. DLT [66] uses the feature points of pixel coordinates and the corresponding 3D points of absolute coordinates in the scene to compute intrinsic and extrinsic parameters based on least square method, while the 3D points of absolute coordinates in the scene are not needed in the five-point algorithm and eight-point algorithm.

3.1.4. Sparse 3D reconstruction

The aim of the step is to compute the 3D locations of points by using the feature points with correspondences obtained from Section 3.1.2 and the camera parameters of each image obtained from Section 3.1.3 to generate a point cloud of the scene.

The algorithm used for the step is called triangulation algorithm [28,29,38,43]. With the matched feature points of each image pair from the feature matching step and the camera parameters of each image from the camera motion estimation step, the 3D locations of the points corresponding to the matched feature points are obtained by the

algorithm, a point cloud of the scene is thus obtained [67].

3.1.5. Model parameters correction

The aim of the step is to correct the camera parameters of each image by using the intrinsic and extrinsic parameters of cameras for each image obtained from Section 3.1.3 and the 3D locations of points in the point cloud obtained from the previous step to generate the precise camera parameters of each image and the precise 3D locations of points in the point cloud.

BA is based on a nonlinear least square method and is used to correct the camera parameters of each image and the 3D location of points in the point cloud [67].

3.1.6. Absolute scale recovery

The aim of the step is to determine the absolute scale of the sparse point cloud obtained from the former step [18] by using the dimensions or points of absolute scale and the local coordinates of points in the sparse point cloud.

Geo-registration is similar to coordinate transformation [51,52]. In the algorithm, the rotation and translation matrices between the sparse point cloud and the points in the absolute geocentric coordinate system are computed. Then, the sparse point cloud is transformed into the absolute geocentric coordinate system by the rotation and translation matrices. In the manual absolute scale recovery method [53], one or more dimensions in the scene are measured manually. Then the absolute scale of the sparse point cloud is obtained based on the relationship between the dimensions in the sparse point cloud and the measured dimensions. In the method of recovery by premeasured objects [53], the corners are reconstructed along with the reconstruction of feature points. Then the absolute scale of the sparse point cloud is obtained based on the relationship between the premeasured dimensions of the objects and the dimensions between the corners in the reconstruction results. Compared to the method of recovery by premeasured objects, the manual absolute scale recovery method is error-prone and reduces the speed of the step of absolute scale recovery.

3.1.7. Dense 3D reconstruction

The aim of the step is to recover the details of the scene, by using the images of a certain scene, the intrinsic and extrinsic parameters of cameras for each image obtained from Section 3.1.5 and the sparse point cloud obtained from the previous step to generate a dense point cloud.

CMVS removes the redundant images of the scene and clusters the resulting images to generate clustered images [29,68]. PMVS uses the clustered images from CMVS and generates a dense 3D point cloud through three steps, namely matching, expansion and filtering [16,29,44]. SGM is utilized to generate dense point cloud based on global energy minimization process [43]. Generally, SGM is faster than PMVS, while the accuracy of results from PMVS is more stable than that from SGM [69].

At present, software applications that implement some of the aforementioned algorithms already exist and can be used to recover scenes, such as VisualSFM [70] and Bundler [71]. Both of the two software applications contain the functions of feature point extraction, feature point matching, camera motion estimation and sparse 3D reconstruction, and they can be used to reconstruct scenes. However, if the software applications do not meet the required accuracy or computation time, aforementioned algorithms or more advanced ones should be implemented to meet the requirements.

3.2. Generating point clouds from stereo images

Compared to the process of generating point clouds from monocular images, the process of generating point clouds from stereo images skips the steps of camera motion estimation and absolute scale recovery and adds a step named binocular camera calibration [20,72] before the step of feature extraction, as shown in Fig. 1.

The aim of binocular camera calibration is to recover the intrinsic parameters of each camera and the extrinsic parameters (rotation and translation) between the two cameras of the binocular camera [38,58]. A two-step procedure is used for binocular camera calibration [20,58]. First, the intrinsic parameters of each camera are estimated by observing a calibration object with known spatial geometry, such as a calibration board [73,74]. Second, the extrinsic parameters are estimated by SfM and can be refined by PMVS and BA [75].

3.3. Generating point clouds from video frames

According to the number of cameras the video cameras use, the process of generating point clouds from video cameras can be classified into two categories: (1) video camera with monocular camera, and (2) video camera with binocular camera. The process of generating point clouds from a video camera with monocular camera is similar to that from monocular cameras, while the process of generating point clouds from a video camera with binocular camera is similar to that from binocular cameras.

Generally, all video frames of video cameras will be used in the process of generating point clouds [20,49,58,76]. However, if a large quantity of video frames is included in the output of the video cameras, it is essential to select key frames for subsequent image processing due to three reasons: (1) too many video frames will increase the time of image processing, (2) the objects for 3D reconstruction techniques only appear in a portion of the video frames, and (3) low quality video frames, such as video frames with motion blur, will reduce the quality of 3D reconstruction results.

Two methods are usually used for key frames selection. The first method is that key frames are selected every other fixed number consecutive video frames in a video [49]. The second method is that key frames are selected when they meet some criteria [19], such as no motion blur and small re-projection errors [77].

4. Techniques for processing point clouds

Generally, the point clouds of objects obtained by using the techniques in Section 3 or from laser scanners cannot meet the application requirements. For example, point clouds contain points from surroundings, which will be an obstacle for further applications of the point clouds. To make the point clouds meet the application requirements, four steps are needed, i.e. point cloud preprocessing, mesh reconstruction, point cloud segmentation and point cloud modeling. The algorithms and methods used in each step and sub-step are shown in Table 4.

Table 4
Algorithms and methods used in the steps for processing point clouds.

Steps	Sub-steps	Algorithms and methods
Point cloud preprocessing	Registration	Iterative Closest Point (ICP) [43,52,78]
	Noise filtering	Removing points manually [79];
	Outlier removal	RANSAC [28]
	Down-sampling	Point spacing strategy [80];
Mesh reconstruction	–	Poisson surface reconstruction (PSR) [29,54,81]
Point cloud segmentation	–	Region growth [82,83]; K-means clustering [78]; Voxel-based algorithm [84]; Hough transform [85]; RANSAC [86]
Point cloud modeling	–	Obtaining the dimensions of objects [79,87,88]

4.1. Point cloud preprocessing

The aims of the step are to generate point cloud models or generate point clouds with high quality for subsequent steps. Generally, the step contains four sub-steps, i.e. registration, noise filtering, outlier removal and down-sampling. It deserves to explain that which of the four sub-steps are needed depends on the application requirements and the quality of the point clouds. For example, if the application requirement is a combined point cloud and the existing point clouds are separate, then registration is required.

Typically, the algorithm used for registration is ICP algorithm [43,52,78], which estimates the rigid transformation between two point clouds iteratively by minimizing the distance between matched points.

Point clouds obtained from Section 3 incorporate not only the points from the objects of interest, but also the points from surroundings [89] (also known as noise points) and outliers [28]. The process of removing noise points and outliers are noise filtering and outlier removing respectively. Generally, the algorithms and methods used for noise filtering can also be used for outlier removing and vice versa, because noise points and outliers are all unwanted points and they are not from the objects of interest. The algorithms and methods used for noise filtering and outlier removing include removing points from surroundings manually [79] and RANSAC [28].

In addition, point cloud registration makes overlapped regions denser, which will reduce the efficiency of subsequent processing. Down-sampling is necessary to solve such problems. The algorithm generally used for down-sampling is point spacing strategy [80], which can reduce points in dense regions. In the method, as an algorithm, a point cloud is arranged into 3D grid cells with equal sizes and points in every single 3D grid cell containing at least one point are reduced until requirements met [90].

4.2. Mesh reconstruction

The aim of the step is to generate a mesh model of the object of interest by using the point cloud obtained from previous step.

Mesh reconstruction is necessary for some application requirements due to two reasons: (1) compared to dense point clouds, mesh models obtained from mesh reconstruction are the better choice for visualization of the objects of interest [29]; (2) mesh models can be used for subsequent applications, such as crack detection [54,81]. Typically, the algorithm used for mesh reconstruction is PSR [29,54,81], which reconstruct a watertight, triangulated approximation to the surface of the object according to its point cloud [91].

4.3. Point cloud segmentation

The aim of the step is to segment a point cloud and obtain the points of the objects of interest. Although algorithms used in publications differ slightly from each other, the algorithms used for point cloud segmentation can be classified into two categories, i.e. algorithms for feature-based segmentation and algorithms for model-based segmentation.

Algorithms for feature-based segmentation segment a point cloud based on the features of each points in the point cloud, while algorithms for model-based segmentation segment a point cloud based on the mathematical models of objects of interest. Therefore, algorithms for feature-based segmentation are preferable when the features of points of objects of interest are distinct from others, while algorithms for model-based segmentation are preferable when mathematical models of objects of interest are known.

4.3.1. Feature-based segmentation

This category of algorithms classifies points with same features into a subset according to the features of these points. The features used in the algorithms for feature-based segmentation include the curvature of the point [80,92,93], the angle between normal vectors [82] and the angle between the normal vector of the point and a unit vector [94].

The algorithms commonly used for feature-based segmentation are region growth [82,83] and clustering, while the voxel-based algorithm [84] is rarely used. In the former algorithm, i.e. region growth, a seed point is selected from the point cloud with predefined criteria. Then all neighboring points meeting the predefined requirements of the seed point are added to the same subset as the seed point. Subsequently, a point satisfying predefined criteria in the subset except the seed point is selected as a new seed point. The process is repeated until no point can be added into the subset. K-means clustering, a kind of the clustering algorithms, is used in the literature [78]. In K-means clustering, each point in the point cloud are classified into one of the clusters of predefined number based on its distances to the clusters' centroid. In the voxel-based algorithm, the space of a point cloud is divided into voxels with equal size, and each voxel contains no point or at least one point. Then voxels containing no points are removed and neighboring voxels with elevation difference less than a threshold are classified into the same subset iteratively. The points contained in the voxels of the same subset are segmented from other points.

4.3.2. Model-based segmentation

This category of algorithms segments a point cloud and obtains points that satisfy the mathematical model of the object of interest. Typically, the mathematical model used in model-based segmentation is a plane equation.

Algorithms used for model-based segmentation are Hough transform and RANSAC [28]. For a regular and simple point cloud, the point cloud can be projected to a plane and then points belonging to a plane perpendicular to the plane can be obtained by Hough transform [85], which is used for extracting lines and line segments in a cluttered point cloud. RANSAC can not only obtain the parameters of the mathematical models of the objects including lines and line segments, but also remove outlier points while obtain the points of the objects of interest from the point cloud [86].

4.4. Point cloud modeling

The aim of the step is to generate a geometric model of the object of interest by using the point cloud segment obtained from the previous step.

In order to generate a geometric model of the object of interest, it is essential to obtain the model parameters based on the results of point cloud segmentation. Generally, the method used for obtaining model parameters is obtaining dimensions of objects. For example, the geometric model of a pipeline of MEP system is regarded as a collection of cylinder segment and thus the radius is one of its model parameters. The radius can be obtained by computing the shortest distance from the centerline to the point cloud of the pipeline obtained from point cloud segmentation [79,87], or by projecting the point cloud of the pipeline onto a plane perpendicular to the centerline of it to generating a resulting circle and computing the radius of the circle [88]. With the model parameters, a geometric model of object of interest can be easily generated.

Although both the mesh models and the geometric models can be used for object visualization, the former can be used for representing crack based on its triangle mesh [54,81], while the latter cannot, because a crack can hardly be represented by using a geometric model.

5. Applications of 3D reconstruction techniques

3D reconstruction techniques have been applied in such areas of civil engineering as buildings [95,96], roads [97–99] and bridges [100]. In order to generalize the applications of 3D reconstruction techniques in civil engineering, the applications are divided according

Table 5
Number of applications of 3D reconstruction techniques in civil engineering.

Application areas	Applications categories	Total
Buildings	Object group reconstruction (18);Object reconstruction (11) ;Component reconstruction (2) ; *Deformation assessment (3);Energy performance assessment (5) ;Crack assessment (2)*	41
Bridges	Object group reconstruction (2);Object reconstruction (2) ; *Disease detection (1)*	5
Roads	Object reconstruction (1); Component reconstruction (3);Below component reconstruction (3) ; *Crack assessment (1)*	8
Others	Object group reconstruction (10); *Crack assessment (1)*	11

Note: The italic font indicated the utilitarian applications of the result from applying 3D reconstruction techniques.

to the scale of applications into four levels, i.e. object group, object, component and below component, which represent the reconstruction objects with different sizes. Let us take bridges as example, 'object group' refers to several bridges, 'object' refers to a bridge, 'component' refers to piers of the bridge and 'below component' refers to crack of these piers. The number of applications in terms of application categories and application areas are summarized as shown in Table 5, in which the utilitarian applications of the result from applying 3D reconstruction techniques also included.

It is obvious that the hottest application category is object group reconstruction. In this section, two typical applications in the category of object group reconstruction, i.e. reconstructing and managing construction sites and reconstructing pipelines of MEP systems, are introduced to illustrate how 3D reconstruction techniques and their outputs of the techniques are used in practice. Then, achievements of the applications of the techniques are summarized from three aspects, i.e. the automation level, the operation time and the accuracy of the outputs of the techniques.

5.1. Reconstructing and managing construction sites

Reconstructing and managing construction sites is the major application of 3D reconstruction techniques in construction sites of civil engineering. Managing construction sites can be divided into two aspects, i.e. monitoring construction sites progress and accessing construction project information.

5.1.1. Reconstructing construction sites

Fathi et al. [58] used video frames from a video camera with binocular camera to reconstruct the construction sites. Feature points in two video frames captured simultaneously from the calibrated video camera with binocular camera were detected respectively using SURF. The feature points between the two video frames were matched, and outlier matched feature points were removed RANSAC. Then, triangulation was used to generate a sparse point cloud of construction sites. However, the resulting sparse point cloud was not enough for visualization purposes. Brilakis et al. [20] proposed a new algorithm for construction sites reconstruction based on the literature [58]. The new algorithm incorporated dense 3D reconstruction besides sparse 3D reconstruction, and the dense point cloud generated from a video frame pair was fused with that from the next video frame pair, which was used to reconstruct the construction sites progressively. Experimental results showed that the average value of the differences between dimensions in the sparse point cloud and corresponding tape measurements in real world was 4.7 mm if the objects were 10 m away from the video camera with binocular camera.

Sung and Kim [38] proposed a fast algorithm for the terrain reconstruction of construction sites. In their approach, images from a binocular camera were divided into small, regular and square sub-regions respectively, and corners of the same number were detected in each sub-region using Fast detector and described by MSD. Then, a two-stage cascade matching algorithm combining single-scale coarse matching and multiple-scale fine matching was used for accelerating MSD matching. After matching, a sparse point cloud was obtained using triangulation with the calibrated parameters of binocular cameras. Finally, a probabilistic model was proposed for dense 3D reconstruction. Experiments indicated that the computation time of MSD-based dense 3D reconstruction was 31 times faster than SURF-based dense 3D reconstruction.

5.1.2. Managing construction sites

Zollmann et al. [52] combined 3D reconstruction techniques and Augmented Reality (AR) to monitor construction site progress. In their study, a system consisting of aerial client, reconstruction client and mobile AR client was developed. Micro Aerial Vehicles (MAV) images obtained from a monocular camera on the aerial client were processed through the reconstruction client based on SfM, and the resulting mesh model as well as the as-planned information of the construction sites were superimposed onto the user's view on the mobile AR client, which visualizes the progress of construction sites for monitoring purposes. Golparvar-Fard et al. [41] used 3D reconstruction techniques to reconstruct construction sites and monitor construction sites progress. In their approach, unordered daily construction images from monocular cameras were processed by using SIFT, ANN, RANSAC, DLT, triangulation, BA and other algorithms [18] to obtain an as-built point cloud of the as-built construction site. Then, the at-built point cloud was compared with Industry Foundation Classes (IFC) based BIM model fused with construction schedule. As a result, the progress deviations with different color were visualized on the 4-dimensional AR model [18,41] for monitoring construction sites progress. The as-built point cloud was generated in few hours, while the progress deviations were computed over a few hours, which can meet the requirement of monitoring construction site progress.

Bae et al. [45] developed a vision-based system named Hybrid 4-Dimensional AR for accessing construction project information. The advantage of the system was that the user's location and orientation were automatically and purely derived by image processing. For this purpose, a point cloud of a construction site was firstly obtained by processing images from a monocular camera using SURF, ANN, RANSAC, five-point algorithm, triangulation, BA. The user just needed to take a photo and upload it to the system, then the system would identify the user's location and orientation through the feature detection of the photo, feature matching with each point in the point cloud and camera motion estimation. In order to achieve accessing construction project information, the photo would be overlaid with the information of the BIM elements in the view of the photo according to the user's location and orientation. Experimental results indicated that it would take about three seconds for localization and the success-ratio of localization was over 98 percent.

5.2. Reconstructing pipelines of MEP systems

Reconstructing pipelines of MEP systems mostly focus on the processing point clouds of pipelines of MEP systems, and almost all point clouds are from laser scanners. In general, reconstructing pipelines of MEP systems can be divided into two aspects, i.e. segmenting point cloud and modeling pipelines of MEP systems.

5.2.1. Segmenting point cloud

Dimitrov and Golparvar-Fard [83] proposed an algorithm for obtaining the point clouds of pipelines of MEP systems from a building point cloud. In their approach, the multiple features of each point in the building point cloud were extracted, including surface normal, directions of max and min curvatures, absolute max and min curvature values and surface roughness indicated by the average and standard deviation distance of the points to a circle fitted for computing the curvature. Then the region growth algorithm is used to reconstruct pipelines of MEP systems. In the algorithm, the point with surface roughness below threshold were selected as a seed point and the points that satisfied the specific roughness threshold were added to the same region as the seed point.

Son et al. [80,92,93] proposed a curvature-based algorithm for obtaining the point clouds of as-built pipelines of MEP systems from laser-scanned data. In their study, the point cloud was segmented by means of region growth based on the normal estimation of each point. Then, 30 points were selected randomly from each segment and the curvature for each point was computed based on fitting a local surface patch. The segment was classified as part of a pipeline if 90 percent of the 30 points had a percent error of computed radii less than a threshold. Experimental results showed that the error of pipeline of MEP systems classification was below 5 percent.

5.2.2. Modeling pipelines of MEP systems

Lee et al. [79,87] proposed an algorithm to model pipelines of MEP systems automatically. In their study, the extraction of the skeleton of entire 3D pipelines of MEP systems by Voronoi diagram-based algorithm and topological thinning algorithm was firstly implemented on the point cloud obtained from laser scanners, and the output was the skeleton points of each pipeline and connectivity between skeleton points. Then, the skeleton points were classified based on feature-based segmentation. The skeleton points were classified into tee pipes based on the feature, i.e. the number of skeleton points connected to them, while the skeleton points were classified into straight pipes based on another feature, i.e. the acute angle formed by a skeleton point and two skeleton points to which it is connected. The remaining skeleton points represented elbow pipes. Finally, the parameters of pipelines of MEP systems were calculated for modeling pipelines of MEP systems. For example, the radius of each pipeline was determined by calculating the shortest distance from each of the extracted skeleton points to the original point cloud. Experimental results showed that the mean relative error of radius estimation was less than 4 percent.

Patil et al. [88] proposed an algorithm for reconstructing and modeling as-built pipelines of MEP systems from the point cloud from laser scanners. In their study, points were segmented based on normal variances between the nearest points in the point cloud, then the mathematical model of cylinder and RANSAC are used to obtain points in cylinders from the segmentation results. After that, each cylinder orientation was estimated based on Gaussian sphere and Hough transform, and the radius of each cylinder was estimated by projecting points onto the plane perpendicular to the cylinder orientation. Finally, as-built pipelines of MEP systems were modeled according to the parameters of cylinders and the connection between cylinders. Experimental results showed that this algorithm could decrease the false detection of cylinders.

Nahangi and Haas [78] presented an algorithm for modeling pipelines of MEP systems and the automated quantification of discrepancies between as-built and as-planned pipelines of MEP systems. In their study, the extraction of the skeleton of entire 3D pipelines of MEP systems was implemented on the point clouds of as-built and as-planned pipelines of MEP systems, and the output was the skeleton points of each pipeline, which was similar to that in the literatures [79,87]. Then, the skeleton points were clustered by means of K-means clustering and hierarchical clustering to be segmented as straight lines. Subsequently, lines were fitted to the segmented skeleton points based on RANSAC. Then the discrepancies between the corresponding lines of as-built pipelines of MEP systems and as-planned pipelines of MEP systems could be obtained by computing the transformation between them, which indicated the discrepancies between as-built and as-planned pipelines of MEP systems. Experimental results showed that the maximum errors for rotational and translational discrepancies estimation were less than 0.15 degree and 1 mm respectively.

Table 6
The automation level of each step in 3D reconstruction techniques.

Steps and sub-steps	Automation level	Steps and sub-steps	Automation level
Feature extraction	+	Registration	+
Feature matching	+	Noise filtering	~
Camera motion estimation	+	Outlier removal	~
Sparse 3D reconstruction	+	Down-sampling	+
Model parameters correction	+	Mesh reconstruction	+
Dense 3D reconstruction	+	Point cloud segmentation	~
Binocular camera calibration	~	Point cloud modeling	+
Absolute scale recovery	~	–	–

Note: (+) achieved, (~) partially achieved.

5.3. Achievements of the applications of the techniques

3D reconstruction techniques have been exploited in such application categories in civil engineering as object group reconstruction, object reconstruction, component reconstruction, below component reconstruction, deformation assessment, energy performance assessment, crack assessment and disease detection, as shown in Table 5. The techniques bring efficiency promotion to the applications.

3D reconstruction techniques contribute successfully to the automation of obtaining 3D representations of objects of interest in civil engineering, as shown in Table 6. Up to now, the process of generating point clouds from monocular images has been automated for some cases in which the step of absolute scale recovery is not needed, while the process of processing point clouds and the process of generating point clouds from stereo images and video frames has been semi-automated.

The operation time of generating point clouds ranges from a few minutes to a few hours, as shown in Table 7, which can meet application requirements of most of the applications. Also, some methods have been used to accelerate the process of generating point clouds, such as GPU and multicore CPU-based implementation of the process, which is about 3 times faster than SfM [49].

The dimension differences of the outputs of 3D reconstruction techniques range from a few millimeters to a few centimeters, as shown in Table 8, which is acceptable for the cases where their application requirements for accuracy is not high. Generally, point clouds from laser scanners have high accuracy, and they are taken as ground truth to determine the accuracy of point clouds generated from monocular images, stereo images and video frames [43,57,67].

6. Future directions

In this section, challenges of applications of 3D reconstruction techniques in civil engineering are discussed, then the key research directions to be addressed in the future are proposed based on the discussion.

Table 7
The operation time of generating point clouds of 3D reconstruction techniques.

Inputs	Outputs	Objects	Image number	Image size	Operation time	Publications
Monocular images	A dense point cloud	A student dining	288	2144 × 1424	A few hours	[41]
		A room	440	2048 × 1536	2 h 21 min	[40,46]
		A room	454		1 h 52 min	[40]
		A room	209		1 h 12 min	[40]
		Terrain surface	30	6732 × 9000	2 h 9 min	[69]
		Highway assets	66	–	1 h 21 min	[49]
			120		6 h 13 min	[98]
	A sparse point cloud	A construction site	125	–	12 min	[45]

Table 8
The accuracy of the outputs of 3D reconstruction techniques.

Inputs	Outputs	Objects	Dimension differences	Publications
Monocular images	A dense point cloud	Indoor space	1.4 mm	[53]
		Outdoor space	2.7 mm	
		A school building	107 mm	[43]
		An electrical substation	7.1 mm	[44]
		Cracks	0.34 mm	[28]
	Dense point clouds	Buildings	20 mm	[57]
	A mesh model	A column	7 mm	[54]
Video frames[1]	A sparse point cloud	A construction site	4.7 mm	[20,58]
Point clouds from laser scanners	A point cloud	Roads	6 mm	[99]
		Pipelines of MEP systems	4 mm	[80]
	A mesh model	Walls	43.6 mm	[86]
	A geometric model	An interchange bridge	190 mm	[84]
		Road junctions	5 mm	[97]
		Pipelines of	2.8 mm	[87]
		MEP systems	3.8 mm	[88]

[1] Video frames from a video camera with binocular cameras.

6.1. Enhancing application areas and application categories

3D reconstruction techniques have been applied in many application areas of civil engineering, such as buildings, bridges and roads, as shown in Table 5. For other areas of civil engineering, such as railways and tunnels, the techniques have been rarely applied. Similarly, application categories of the techniques are mainly object group reconstruction and object reconstruction, while other application categories of the techniques are rare, such as component reconstruction and below component reconstruction. Because the application requirement of obtaining 3D representations of objects of interest exists in aforementioned areas and application categories, enhancing applications of the techniques in those areas and application categories is expected.

6.2. Reconstructing subsurface

Generally, the outputs of 3D reconstruction techniques are 3D representations of the surface of objects of interest, such as point cloud models, mesh models and geometric models. The techniques have been rarely applied for obtaining 3D representations of the internal structure of objects. However, obtaining 3D representations of the internal structure of objects is essential especially for objects with concealed work, such as reinforced skeleton frame. With the 3D representations of the internal structure of objects, not only dimensions of the internal structure of objects can be obtained, but also stress analysis and other applications can be implemented. Therefore, subsurface reconstruction is expected for the applications of the techniques in the future.

6.3. Upgrading automation level

The process of 3D reconstruction techniques has not been fully automated as shown in Table 6. Some methods used in the steps for processing point clouds are still manual or semi-automated, which increases the operation time of the techniques and makes obtaining 3D representations error-prone. For example, the methods used for noise filtering and outlier removal are generally manual, and the methods need to be improved to be automated.

6.4. Reducing operation time

Although the operation time of 3D reconstruction techniques is acceptable for most of the applications as shown in Table 7, the techniques need to be accelerated for real-time applications, such as the applications with AR. The operation time of the techniques depends on the two aspects: (1) the amount of inputs of the techniques; (2) operation time of each step of the techniques. Increasing the amount of the inputs of the techniques, such as monocular images, can improve the accuracy the outputs of the techniques. However, the increasing inputs increase the operation time of the techniques. The manual or semi-automated steps and the steps needing much time impede the acceleration of the techniques.

6.5. Improving accuracy

Up to now, the accuracy of 3D reconstruction techniques is acceptable for the applications as shown in Table 8. But for other applications whose application requirements for accuracy are high, such as quality detection of reinforced skeleton frame and ground settlement assessment, existing algorithms and methods should be improved for high accuracy. The accuracy of the techniques depends on two aspects: (1) the quality of inputs from data collection equipment, such as image resolution; (2) the accuracy of the algorithms and methods used for generating point clouds and processing point clouds. In order to improve the accuracy of the techniques, efforts should be made to improve the two aspects.

In summary, it is concluded that the techniques are currently not possible to obtain 3D representations of objects of interest with high speed, high accuracy and full automation at the same time. Therefore, more studies need to be conducted to improve the algorithms and methods for enlarging the applications of 3D reconstruction techniques in civil engineering.

The key research directions that have to be addressed in the future are highlighted in the following list to enlarge the applications of 3D reconstruction techniques in civil engineering:

(1) What application areas and categories of the techniques can we enhance? And how can we enhance them?
(2) How can we fulfill the subsurface reconstruction by using the techniques? How to utilize other data collection equipment, such as

ultrasonic tomography and CT, to obtain 3D representations of internal structure of objects of interest? How to combine monocular cameras, binocular cameras, video cameras or laser scanners with ultrasonic tomography or CT to obtain surface and subsurface 3D representations of objects of interest, which can facilitate the applications of the techniques for more complicated assessment or analysis?

(3) How can we upgrade the automation level of the techniques? For example, how to improve the manual and semi-automated steps of the techniques to achieve the goal?

(4) How can we accelerate the techniques to meet the high application requirement for operation time? For example, how to improve the steps needing much time to achieve the goal? How to reduce the amount of inputs for the techniques to achieve the goal? How to utilize artificial intelligent techniques to improve the steps needing much time or reduce the amount of inputs for the techniques?

(5) How can we improve the accuracy of the outputs of the techniques to meet the high application requirement for accuracy? For example, how to improve the algorithms and methods used for the techniques to achieve the goal? How to utilize different data collection equipment or artificial intelligent techniques to improve the quality of inputs of 3D reconstruction techniques to achieve the goal?

7. Conclusions

3D reconstruction techniques have brought convenience for obtaining 3D representations of objects of interest and thus have been used for many applications in many areas. However, the applications of the techniques in civil engineering are still in the early stage. More studies need to be conducted to make the techniques meet high application requirements, such as full automation, high accuracy and less operation time.

This paper reviews the 3D reconstruction techniques in civil engineering and their achievements and challenges. The method of literature retrieval and determining research scope was determined. By analyzing the retrieved papers, 3D reconstruction techniques for generating point clouds and processing point clouds along with the corresponding algorithms and methods were presented respectively. The application of 3D reconstruction techniques for reconstructing and managing construction sites and for reconstructing pipelines of MEP systems were introduced as typical examples, and the achievements of the applications of the 3D reconstruction techniques in civil engineering was summarized. Finally, the challenges of the applications of the techniques in civil engineering were discussed and the key research directions to be addressed in the future were proposed.

This paper contributes to the knowledge body of 3D reconstruction in two aspects, i.e. summarizing systematically the up-to-date achievements and challenges for the applications of 3D reconstruction techniques in civil engineering, and proposing key future research directions to be addressed in the field.

Conflict of interest

There are no conflicts to declare.

Acknowledgements

This study is supported by the 'National Natural Science Foundation of China' (No. 51678345).

References

[1] 3-D reconstruction, < https://www.nature.com/subjects/3d-reconstruction > (accessed: 2018-03-02).
[2] 3D reconstruction, < https://en.wikipedia.org/wiki/3D_reconstruction > (accessed: 2018-03-02).
[3] Q. Lu, S. Lee, Image-based technologies for constructing as-is building information models for existing buildings, J. Comput. Civil Eng. 31 (4) (2017).
[4] E. Kwak, I. Detchev, A. Habib, M. El-Badry, C. Hughes, Precise photogrammetric reconstruction using model-based image fitting for 3D beam deformation monitoring, J. Surv. Eng. 139 (3) (2013) 143–155.
[5] L. Humbert, J.A. De Guise, B. Aubert, B. Godbout, W. Skalli, 3D reconstruction of the spine from biplanar X-rays using parametric models based on transversal and longitudinal inferences, Med. Eng. Phys. 31 (6) (2009) 681–687.
[6] X. Lu, Y. Wang, Y. Lu, X. Ge, B. Song, Qiyun pagoda 3D model reconstruction based on laser cloud data, Bulletin of Surveying and Mapping 9 (2011) 11–14 (in Chinese).
[7] X. Brunetaud, L. De Luca, S. Janvier-Badosa, K. Beck, M. Al-Mukhtar, Application of digital techniques in monument preservation, Eur. J. Environ. Civil Eng. 16 (5) (2012) 543–556.
[8] P. Ren, W. Wang, X. Bai, Reconstruction of imperial university of shanxi based on virtual reality technology, Comput. Simul. 29 (11) (2012) 20–23 (in Chinese).
[9] Y. Ham, M. Golparvar-Fard, Three-dimensional thermography-based method for cost-benefit analysis of energy efficiency building envelope retrofits, J. Comput. Civil Eng. 29 (4) (2015).
[10] Y. Liu, S. Han, O. Xu, Acquisition system for three-dimensional surface texture of asphalt pavement based on digital image processing, J. Southwest Jiaotong Univ. 49 (2) (2014) 351–357 (in Chinese).
[11] P. Tang, D. Huber, B. Akinci, R. Lipman, A. Lytle, Automatic reconstruction of as-built building information models from laser-scanned point clouds: a review of related techniques, Autom. Constr. 19 (7) (2010) 829–843.
[12] E.A. Parn, D. Edwards, Vision and advocacy of optoelectronic technology developments in the AECO sector, Built Environ. Proj. Asset Manage. 7 (3) (2017) 330–348.
[13] H. Son, F. Bosche, C. Kim, As-built data acquisition and its use in production monitoring and automated layout of civil infrastructure: a survey, Adv. Eng. Inf. 29 (2) (2015) 172–183.
[14] J. Teizer, Status quo and open challenges in vision-based sensing and tracking of temporary resources on infrastructure construction sites, Adv. Eng. Inf. 29 (2) (2015) 225–238.
[15] C. Koch, K. Georgieva, V. Kasireddy, B. Akinci, P. Fieguth, A review on computer vision based defect detection and condition assessment of concrete and asphalt civil infrastructure, Adv. Eng. Inf. 29 (2) (2015) 196–210.
[16] C. Koch, S.G. Paal, A. Rashidi, Z. Zhu, M. Konig, I. Brilakis, Achievements and challenges in machine vision-based inspection of large concrete structures, Adv. Struct. Eng. 17 (3) (2014) 303–318.
[17] S. Mathavan, K. Kamal, M. Rahman, A review of three-dimensional imaging technologies for pavement distress detection and measurements, IEEE Trans. Intell. Transport. Syst. 16 (5) (2015) 2353–2362.
[18] M. Golparvar-Fard, F. Pena-Mora, S. Savarese, D4AR - a 4-dimensional augmented reality model for automating construction progress monitoring data collection, processing and communication, Electron. J. Inform. Technol. Constr. 14 (2009) 129–153.
[19] V. Balali, M. Golparvar-Fard, J.M. De La Garza, Video-based highway asset recognition and 3D localization, in: Computing in Civil Engineering – Proceedings of the 2013 ASCE International Workshop on Computing in Civil Engineering, 2013, pp. 379–386.
[20] I. Brilakis, H. Fathi, A. Rashidi, Progressive 3D reconstruction of infrastructure with videogrammetry, Autom. Constr. 20 (7) (2011) 884–895.
[21] G.M. Jog, H. Fathi, I. Brilakis, Automated computation of the fundamental matrix for vision based construction site applications, Adv. Eng. Inf. 25 (4) (2011) 725–735.
[22] N. Benmansour, R. Labayrade, D. Aubert, S. Glaser, D. Gruyer, A model driven 3D lane detection system using stereovision, in: 2008 10th International Conference on Control, Automation, Robotics and Vision, ICARCV 2008, 2008, pp. 1277–1282.
[23] Y.C. Tsai, Z.Z. Hu, Z.H. Wang, Vision-based roadway geometry computation, J. Transport. Eng. – Asce 136 (3) (2010) 223–233.
[24] M. Hofer, A. Wendel, H. Bischof, Incremental line-based 3D reconstruction using geometric constraints, in: BMVC 2013 – Electronic Proceedings of the British Machine Vision Conference 2013, 2013, pp. Dyson; HP; IET Journals – The Institution of Engineering and Technology; Microsoft Research; Qualcomm.
[25] M. Hofer, M. Maurer, H. Bischof, Line3d: efficient 3D scene abstraction for the built environment, in: Lecture Notes in Computer Science (including subseries Lecture Notes in Artificial Intelligence and Lecture Notes in Bioinformatics), 2015, pp. 237–248.
[26] Z.-Z. Hu, L. Zhang, D.-F. Bai, B. Zhao, Computation of road curvature from a sequence of consecutive in-vehicle images, J. Transport. Syst. Eng. Inform. Technol. 16 (1) (2016) 38–45 (in Chinese).
[27] M. Hofer, M. Maurer, H. Bischof, Efficient 3D scene abstraction using line segments, Comput. Vis. Image Underst. 157 (2017) 167–178.
[28] Y.F. Liu, S. Cho, B.F. Spencer, J.S. Fan, Concrete crack assessment using digital image processing and 3D scene reconstruction, J. Comput. Civil Eng. 30 (1) (2016).
[29] M.D. Yang, C.F. Chao, K.S. Huang, L.Y. Lu, Y.P. Chen, Image-based 3D scene reconstruction and exploration in augmented reality, Autom. Constr. 33 (2013) 48–60.
[30] D.G. Lowe, Distinctive image features from scale-invariant keypoints, Int. J. Comput. Vision 60 (2) (2004) 91–110.
[31] H. Bay, T. Tuytelaars, L. Van Gool, SURF: speeded up robust features, in: Lecture Notes in Computer Science (including subseries Lecture Notes in Artificial Intelligence and Lecture Notes in Bioinformatics), 2006, pp. 404–417.
[32] H. Bay, A. Ess, T. Tuytelaars, L. Van Gool, Speeded-up robust features (SURF),

Comput. Vis. Image Underst. 110 (3) (2008) 346–359.
[33] J.-M. Morel, G. Yu, ASIFT: a new framework for fully affine invariant image comparison, SIAM J. Imag. Sci. 2 (2) (2009) 438–469.
[34] F. Huang, Z. Mao, W. Shi, ICA-ASIFT-based multi-temporal matching of high-resolution remote sensing urban images, Cybern. Inform. Technol. 16 (5) (2016) 34–49.
[35] C. Harris, M. Stephens, A combined corner and edge detector, Proc. Alvey. Vision Conf. 3 (1988) 147–151.
[36] E. Rosten, T. Drummond, Machine learning for high-speed corner detection, in: Lecture Notes in Computer Science (including subseries Lecture Notes in Artificial Intelligence and Lecture Notes in Bioinformatics), 2006, pp. 430–443.
[37] A. Alahi, R. Ortiz, P. Vandergheynst, FREAK: fast retina keypoint, in: Proceedings of the IEEE Computer Society Conference on Computer Vision and Pattern Recognition, 2012, pp. 510–517.
[38] C. Sung, P.Y. Kim, 3D terrain reconstruction of construction sites using a stereo camera, Autom. Constr. 64 (2016) 65–77.
[39] J. Wang, L. Zhu, 3D building facade reconstruction based on image matching-point cloud fusing, Chin. J. Comput. 35 (10) (2012) 2072–2079 (in Chinese).
[40] Y. Ham, M. Golparvar-Fard, EPAR: energy performance augmented reality models for identification of building energy performance deviations between actual measurements and simulation results, Energy Build. 63 (2013) 15–28.
[41] M. Golparvar-Fard, F. Pena-Mora, S. Savarese, Automated progress monitoring using unordered daily construction photographs and IFC-based building information models, J. Comput. Civil Eng. 29 (1) (2015).
[42] X. Chen, X. Chen, C. Zhao, Z. He, Design and implementation of unmanned aerial vehicle in the bridge and road disease detection, Bull. Surv. Mapp. 4 (2016) 79–82 (in Chinese).
[43] A. Khaloo, D. Lattanzi, Hierarchical dense structure-from-motion reconstructions for infrastructure condition assessment, J. Comput. Civil Eng. 31 (1) (2017).
[44] P. Rodriguez-Gonzalvez, D. Gonzalez-Aguilera, G. Lopez-Jimenez, I. Picon-Cabrera, Image-based modeling of built environment from an unmanned aerial system, Autom. Constr. 48 (2014) 44–52.
[45] H. Bae, M. Golparvar-Fard, J. White, High-precision and infrastructure-independent mobile augmented reality system for context-aware construction and facility management applications, in: Computing in Civil Engineering – Proceedings of the 2013 ASCE International Workshop on Computing in Civil Engineering, 2013, pp. 637–644.
[46] M. Golparvar-Fard, Y. Ham, Automated diagnostics and visualization of potential energy performance problems in existing buildings using energy performance augmented reality models, J. Comput. Civil Eng. 28 (1) (2014) 17–29.
[47] X. Du, Y.-F. Zhu, A flexible method for 3D reconstruction of urban building, in: International Conference on Signal Processing Proceedings, ICSP, 2008, pp. 1355–1359.
[48] A. Rashidi, F. Dai, I. Brilakis, P. Vela, Comparison of camera motion estimation methods for 3D reconstruction of infrastructure, in: Congress on Computing in Civil Engineering, Proceedings, 2011, pp. 363–371.
[49] M. Golparvar-Fard, V. Balali, J.M. de la Garza, Segmentation and recognition of highway assets using image-based 3D point clouds and semantic texton forests, J. Comput. Civil Eng. 29 (1) (2015).
[50] W. Zhang, Y.K. Zhang, Z. Li, Z. Zheng, R. Zhang, J.X. Chen, A rapid evaluation method of existing building applied photovoltaic (BAPV) potential, Energy Build. 135 (2017) 39–49.
[51] A. Irschara, C. Hoppe, H. Bischof, S. Kluckner, Efficient structure from motion with weak position and orientation priors, in: 2011 IEEE Computer Society Conference on Computer Vision and Pattern Recognition Workshops, 2011, pp. 8.
[52] S. Zollmann, C. Hoppe, S. Kluckner, C. Poglitsch, H. Bischof, G. Reitmayr, Augmented reality for construction site monitoring and documentation, Proc. IEEE 102 (2) (2014) 137–154.
[53] A. Rashidi, I. Brilakis, P. Vela, Generating absolute-scale point cloud data of built infrastructure scenes using a monocular camera setting, J. Comput. Civil Eng. 29 (6) (2015).
[54] M.M. Torok, M. Golparvar-Fard, K.B. Kochersberger, Image-based automated 3D crack detection for post-disaster building assessment, J. Comput. Civil Eng. 28 (5) (2014).
[55] Y. Ham, M. Golparvar-Fard, Mapping actual thermal properties to building elements in gbXML-based BIM for reliable building energy performance modeling, Autom. Constr. 49 (2015) 214–224.
[56] Y. Ham, M. Golparvar-Fard, Identification of potential areas for building retrofit using thermal digital imagery and CFD models, in: Congress on Computing in Civil Engineering, Proceedings, 2012, pp. 642–649.
[57] Z.X. Zhou, J. Gong, M.Y. Guo, Image-based 3D reconstruction for posthurricane residential building damage assessment, J. Comput. Civil Eng. 30 (2) (2016).
[58] H. Fathi, I. Brilakis, P. Vela, Automated 3D structure inference of civil infrastructure using a stereo camera set, in: Congress on Computing in Civil Engineering, Proceedings, 2011, pp. 118–125.
[59] C. Sung, M.J. Chung, Multi-scale descriptor for robust and fast camera motion estimation, ISPL 20 (7) (2013) 725–728.
[60] M. Muja, D.G. Lowe, Scalable nearest neighbor algorithms for high dimensional data, IEEE Trans. Pattern Anal. Mach. Intell. 36 (11) (2014) 2227–2240.
[61] Wikipedia, Random Sample Consensus, < https://en.wikipedia.org/wiki/Random_sample_consensus > (accessed: 2017-12-24).
[62] L. Moisan, B. Stival, A probabilistic criterion to detect rigid point matches between two images and estimate the fundamental matrix, Int. J. Comput. Vision 57 (3) (2004) 201–218.
[63] S. Birchfield, Essential and fundamental matrices, < http://ai.stanford.edu/~birch/projective/node20.html > (accessed: 2018-03-02).
[64] D. Nister, An efficient solution to the five-point relative pose problem, in: Proceedings of the IEEE Computer Society Conference on Computer Vision and Pattern Recognition, 2003, pp. II/195–II/202.
[65] R.I. Hartley, In defense of the eight-point algorithm, IEEE Trans. Pattern Anal. Mach. Intell. 19 (6) (1997) 580–593.
[66] D. Wang, J. Luo, Y. Hu, S. Xie, The method of direct liner transformation on the camera calibration, Mach. Electron. 9 (2006) 9–11 (in Chinese).
[67] B. Bhadrakom, K. Chaiyasarn, As-built 3D modeling based on structure from motion for deformation assessment of historical buildings, Int. J. Geomate 11 (24) (2016) 2378–2384.
[68] Y. Furukawa, B. Curless, S.M. Seitz, R. Szeliski, Towards internet-scale multi-view stereo, in: Proceedings of the IEEE Computer Society Conference on Computer Vision and Pattern Recognition, 2010, pp. 1434–1441.
[69] W. Yuan, S. Chen, Y. Zhang, J. Gong, R. Shibasaki, An aerial-image dense matching approach based on optical flow field, in: International Archives of the Photogrammetry, Remote Sensing and Spatial Information Sciences – ISPRS Archives, 2016, pp. 543–548.
[70] C. Wu, VisualSFM: a visual structure from motion system, < http://ccwu.me/vsfm/ > (accessed: 2017-09-12).
[71] N. Snavely, Bundler: Structure from Motion (SfM) for Unordered Image Collections, < https://www.cs.cornell.edu/~snavely/bundler/ > (accessed: 2017-09-12).
[72] M. Havlena, T. Pajdla, K. Comelis, Structure from omnidirectional stereo rig motion for city modeling, in: VISAPP 2008 – 3rd International Conference on Computer Vision Theory and Applications, Proceedings, 2008, pp. 407–414.
[73] H. Fathi, I. Brilakis, A transformational approach to explicit stereo camera calibration for improved euclidean accuracy of infrastructure 3D reconstruction, in: Computing in Civil Engineering – Proceedings of the 2013 ASCE International Workshop on Computing in Civil Engineering, 2013, pp. 709–716.
[74] H. Fathi, I. Brilakis, Multistep explicit stereo camera calibration approach to improve euclidean accuracy of large-scale 3D reconstruction, J. Comput. Civil Eng. 30 (1) (2016).
[75] Y. Furukawa, J. Ponce, Accurate camera calibration from multi-view stereo and bundle adjustment, Int. J. Comput. Vision 84 (3) (2009) 257–268.
[76] G.M. Jog, C. Koch, M. Golparvar-Fard, I. Brilakis, Pothole properties measurement through visual 2D recognition and 3D reconstruction, in: Congress on Computing in Civil Engineering, Proceedings, 2012, pp. 553–560.
[77] A. Rashidi, F. Dai, I. Brilakis, P. Vela, A novel approach for automated selection of key video frames for 3D reconstruction of civil infrastructure, in: Congress on Computing in Civil Engineering, Proceedings, 2012, pp. 188–195.
[78] M. Nahangi, C.T. Haas, Skeleton-based discrepancy feedback for automated realignment of industrial assemblies, Autom. Constr. 61 (2016) 147–161.
[79] J. Lee, C. Kim, H. Son, C. Kim, Skeleton-based 3D reconstruction of as-built pipelines from laser-scanned data, in: Congress on Computing in Civil Engineering, Proceedings, 2012, pp. 245–252.
[80] H. Son, C. Kim, C. Kim, Fully automated as-built 3D pipeline extraction method from laser-scanned data based on curvature computation, J. Comput. Civil Eng. 29 (4) (2015).
[81] M.M. Torok, M.G. Fard, K.B. Kochersberger, Post-disaster robotic building assessment: automated 3D crack detection from image-based reconstructions, in: Congress on Computing in Civil Engineering, Proceedings, 2012, pp. 397–404.
[82] S. Wang, Q. Gou, M. Sun, Simple building reconstruction from lidar data and aerial imagery, in: 2012 2nd International Conference on Remote Sensing, Environment and Transportation Engineering, RSETE 2012 – Proceedings, 2012.
[83] A. Dimitrov, M. Golparvar-Fard, Segmentation of building point cloud models including detailed architectural/structural features and MEP systems, Autom. Constr. 51 (2015) 32–45.
[84] L. Cheng, Y. Wu, Y. Wang, L. Zhong, Y. Chen, M. Li, Three-dimensional reconstruction of large multilayer interchange bridge using airborne LiDAR data, IEEE J. Sel. Top. Appl. Earth Obs. Remote Sens. 8 (2) (2015) 691–708.
[85] A. Adan, D. Huber, 3D reconstruction of interior wall surfaces under occlusion and clutter, in: Proceedings – 2011 International Conference on 3D Imaging, Modeling, Processing, Visualization and Transmission, 3DIMPVT 2011, 2011, pp. 275–281.
[86] E. Valero, A. Adan, F. Bosche, Semantic 3D reconstruction of furnished interiors using laser scanning and RFID technology, J. Comput. Civil Eng. 30 (4) (2016).
[87] J. Lee, H. Son, C. Kim, C. Kim, Skeleton-based 3D reconstruction of as-built pipelines from laser-scan data, Autom. Constr. 35 (2013) 199–207.
[88] A.K. Patil, P. Holi, S.K. Lee, Y.H. Chai, An adaptive approach for the reconstruction and modeling of as-built 3D pipelines from point clouds, Autom. Constr. 75 (2017) 65–78.
[89] L. Yang, Y. Sheng, B. Wang, 3D reconstruction for indoor-outdoor architecture based on 3D laser scanning, Bul. Surv. Mapp. 7 (2014) 27–30 (in Chinese).
[90] Y. Li, H. Wu, H. Xu, R. An, J. Xu, Q. He, A gradient-constrained morphological filtering algorithm for airborne LiDAR, Opt. Laser Technol. 54 (2013) 288–296.
[91] K. Michael, B. Matthew, H. Hugues, Poisson surface reconstruction, Eurographics Symposium on Geometry Processing, 2006, pp. 61–70.
[92] H. Son, C. Kim, C. Kim, Fully automated as-built 3D pipeline segmentation based on curvature computation from laser-scanned data, in: Computing in Civil Engineering – Proceedings of the 2013 ASCE International Workshop on Computing in Civil Engineering, 2013, pp. 765–772.
[93] H. Son, C. Kim, C. Kim, 3D reconstruction of as-built industrial instrumentation models from laser-scan data and a 3D CAD database based on prior knowledge, Autom. Constr. 49 (2015) 193–200.
[94] Q. Zhan, L. Yu, Objects classification from laser scanning data based on multi-class support vector machine, in: 2011 International Conference on Remote Sensing, Environment and Transportation Engineering, RSETE 2011 – Proceedings, 2011, pp. 520–523.

[95] G. Sourimant, L. Morin, K. Bouatouch, GPS, GIS and video registration for building reconstruction, in: Proceedings – International Conference on Image Processing, ICIP, 2006, pp. VI401–VI404.
[96] J. Zhao, D. Li, Y. Wang, Ancient architecture point cloud data segmentation based on modified fuzzy c-means clustering algorithm, in: Proceedings of SPIE – The International Society for Optical Engineering, 2008.
[97] S.J. Oude Elberink, G. Vosselman, 3D information extraction from laser point clouds covering complex road junctions, Photogramm. Rec. 24 (125) (2009) 23–36.
[98] B. Uslu, M. Golparvar-Fard, J.M. De La Garza, Image-based 3D reconstruction and recognition for enhanced highway condition assessment, in: Congress on Computing in Civil Engineering, Proceedings, 2011, pp. 67–76.
[99] F.A. Moreno, J. Gonzalez-Jimenez, J.L. Blanco, A. Esteban, An instrumented vehicle for efficient and accurate 3D mapping of roads, Comput. – Aided Civ. Infrastruct. Eng. 28 (6) (2013) 403–419.
[100] D. Lattanzi, G.R. Miller, 3D scene reconstruction for robotic bridge inspection, J. Infrastruct. Syst. 21 (2) (2015).